Seminar at ECT* - workshop Nonequilibrium phenomena in superfluid systems

Determining Fission Fragment Spin Properties Using Projection Techniques

Guillaume SCAMPS

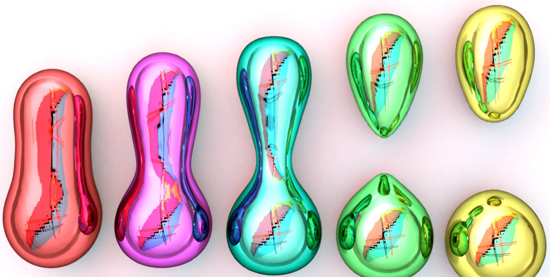

UNIVERSITÉ DE TOULOUSE

L2IT

cnrs

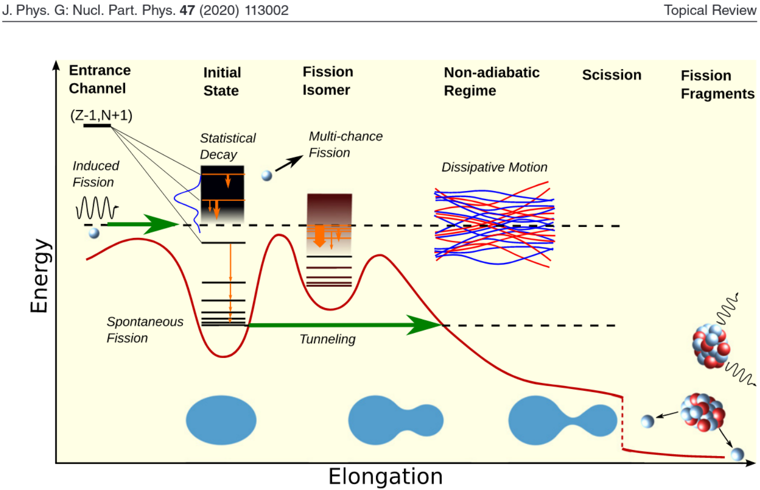
J. Phys. G: Nucl. Part. Phys. 47 (2020) 113002
Topical Review
Entrance Channel
Initial State
Fission Isomer
Non-adiabatic Regime
Scission
Fission Fragments
(Z-1,N+1)
Statistical Decay
Multi-chance Fission
Induced Fission
Dissipative Motion
Energy
Spontaneous Fission
Tunneling
Elongation

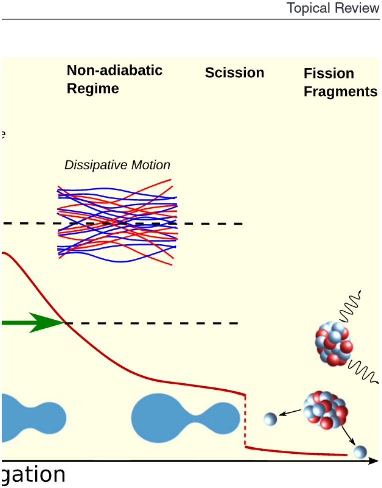
Topical Review
Non-adiabatic Regime
Scission
Fission Fragments
Dissipative Motion
gation

What do we want to understand ?

- Charge and mass distribution
- Connection with structure
- Odd-even effects
- Charge polarization
- Spin of the fragments

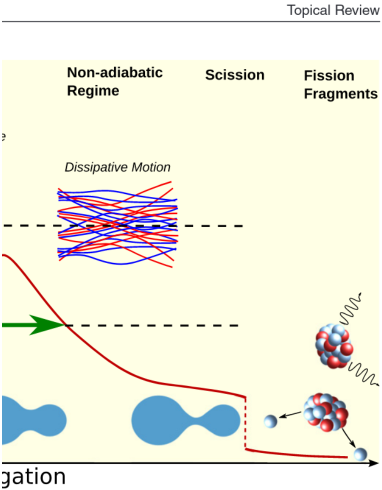

Why do we need pairing ?

Fission barrier : ^{258}Fm

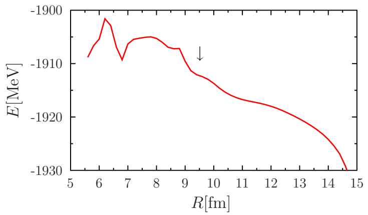

TDHF

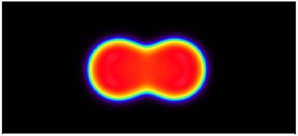

TDHF+BCS

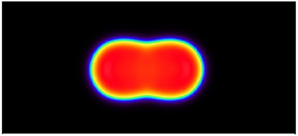

G. Scamps, C. Simenel, D. Lacroix, PRC **92**, 011602(R) (2015).

Fission barrier : ^{258}Fm

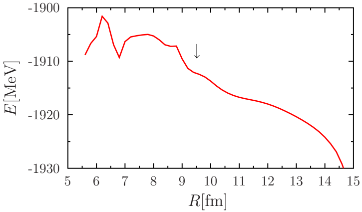

TDHF

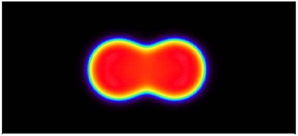

TDHF+BCS

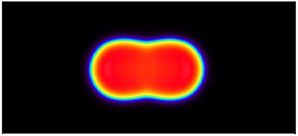

G. Scamps, C. Simenel, D. Lacroix, PRC **92**, 011602(R) (2015).

Fission barrier : ^{258}Fm

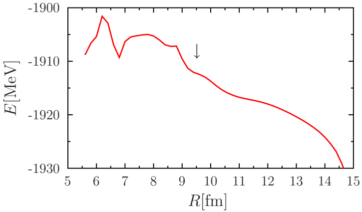

TDHF

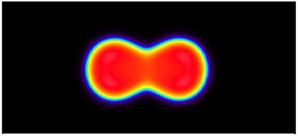

TDHF+BCS

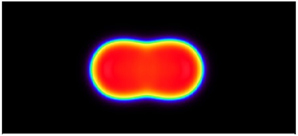

G. Scamps, C. Simenel, D. Lacroix, PRC **92**, 011602(R) (2015).

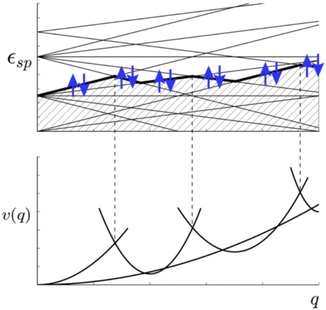

TDHF

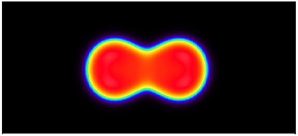

TDHF+BCS

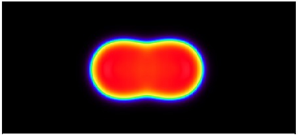

G. Scamps, C. Simenel, D. Lacroix, PRC **92**, 011602(R) (2015).

Impact of pairing

Pairing is a lubricant for fission

Quasi-particle vacuum

$$|\Psi\rangle = \prod_{\alpha}(u_\alpha + v_\alpha a^\dagger_\alpha a^\dagger_{\bar{\alpha}})|-\rangle$$

In the particular case of two particles and two states :

$$\begin{aligned} |\Psi\rangle &= (u_1 + v_1 a^\dagger_1 a^\dagger_{\bar{1}})(u_2 + v_2 a^\dagger_2 a^\dagger_{\bar{2}})|-\rangle \\ &= u_1 u_2|-\rangle + u_2 v_1 a^\dagger_1 a^\dagger_{\bar{1}}|-\rangle + u_1 v_2 a^\dagger_2 a^\dagger_{\bar{2}}|-\rangle + v_1 v_2 a^\dagger_1 a^\dagger_{\bar{1}} a^\dagger_2 a^\dagger_{\bar{2}}|-\rangle \end{aligned}$$

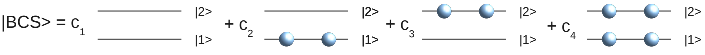

Projector on the good number of particles

$$\hat{P}(N) = \frac{1}{2\pi}\int_0^{2\pi} e^{i\varphi(\hat{N}-N)}d\varphi$$

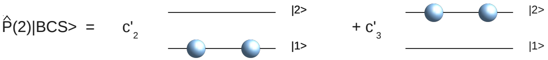

Projection technique (C. Simenel, PRL 105 (2010))

$$\hat{P}_B(N) = \frac{1}{2\pi}\int_0^{2\pi} e^{i\varphi(\hat{N}_B - N)} d\varphi$$

$$P_B(N) = \langle\Psi(t)|\,\hat{P}_B(N)|\Psi(t)\rangle$$

^{48}Ca + ^{40}Ca

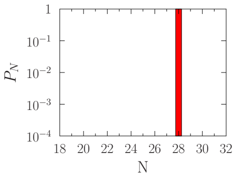

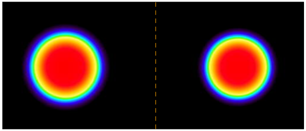

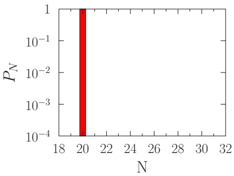

Transfer probability

Projection technique (C. Simenel, PRL 105 (2010))

$$\hat{P}_B(N) = \frac{1}{2\pi}\int_0^{2\pi} e^{i\varphi(\hat{N}_B - N)}\,d\varphi$$

$$P_B(N) = \langle\Psi(t)|\,\hat{P}_B(N)|\Psi(t)\rangle$$

$^{48}Ca + {}^{40}Ca$

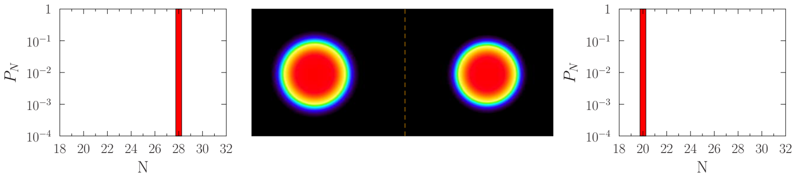

Same projection technique for a BCS state

$$|\Psi(t)\rangle = |\phi_1\rangle \otimes |\phi_2\rangle = \prod_{\alpha_1}(u_{\alpha_1} + v_{\alpha_1} a^\dagger_{\alpha_1} a^\dagger_{\hat{\alpha}_1}) \prod_{\alpha_2}(u_{\alpha_2} + v_{\alpha_2} a^\dagger_{\alpha_2} a^\dagger_{\hat{\alpha}_2})|-\rangle$$

$$\hat{P}_B(N) = \frac{1}{2\pi}\int_0^{2\pi} e^{i\varphi(\hat{N}_B - N)} d\varphi$$

$$P_B(N) = \langle\Psi(t)|\ \hat{P}_B(N)|\Psi(t)\rangle$$

^{46}Ca + ^{40}Ca

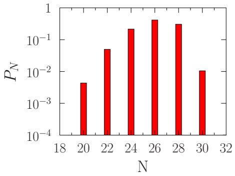

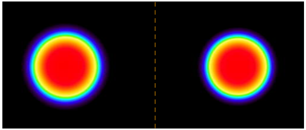

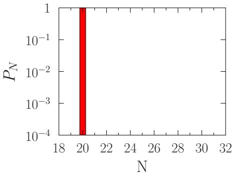

Same projection technique for a BCS state

$$|\Psi(t)\rangle = |\phi_1\rangle \otimes |\phi_2\rangle = \prod_{\alpha_1}(u_{\alpha_1} + v_{\alpha_1} a^\dagger_{\alpha_1} a^\dagger_{\hat{\alpha}_1}) \prod_{\alpha_2}(u_{\alpha_2} + v_{\alpha_2} a^\dagger_{\alpha_2} a^\dagger_{\hat{\alpha}_2})|-\rangle$$

$$\hat{P}_B(N) = \frac{1}{2\pi}\int_0^{2\pi} e^{i\varphi(\hat{N}_B - N)} d\varphi$$

$$P_B(N) = \langle\Psi(t)|\ \hat{P}_B(N)|\Psi(t)\rangle$$

^{46}Ca + ^{40}Ca

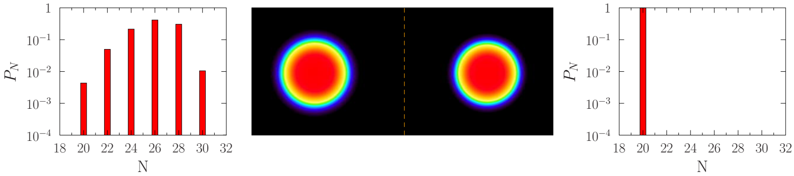

Double projection technique for a BCS state

$$P_B(N) = \frac{\langle\Psi(t)|\hat{P}_B(N)\hat{P}(N_0)|\Psi(t)\rangle}{\langle\Psi(t)|\hat{P}(N_0)|\Psi(t)\rangle}$$

^{46}Ca + ^{40}Ca

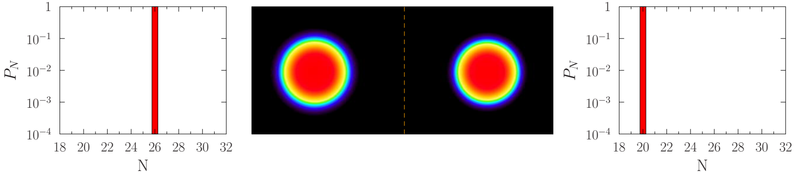

Transfer probability

Double projection technique for a BCS state

$$P_B(N) = \frac{\langle \Psi(t) | \hat{P}_B(N) \hat{P}(N_0) | \Psi(t) \rangle}{\langle \Psi(t) | \hat{P}(N_0) | \Psi(t) \rangle}$$

^{46}Ca + ^{40}Ca

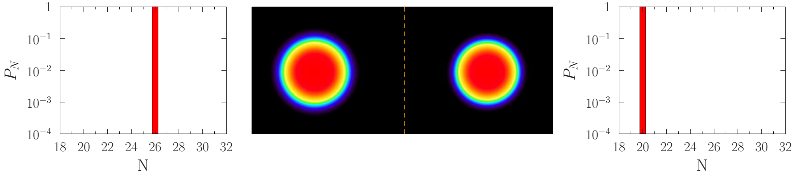

Effect of pairing on P_1 and P_2

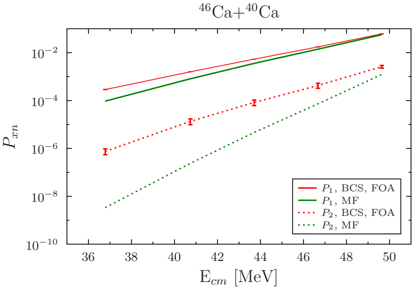

Effect of initial pairing correlations :

- fragmentation of single particle occupation numbers
  - enhancement of P_{1n}
- non-zero two body correlations ($\kappa \neq 0$)
  - enhancement of P_{2n}

G. Scamps and D. Lacroix, PRC 87, (2013)

Spins of the fission fragments

Spin of the fragments

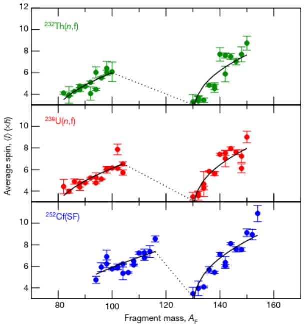

Correlations

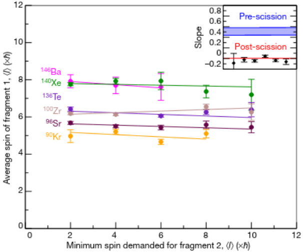

J. N. Wilson, Nature, 590, 566 (2021)

- The average spin follows a sawtooth shape
- No correlations between the spins of the fragments

Spins are mostly perpendicular to the fission axis

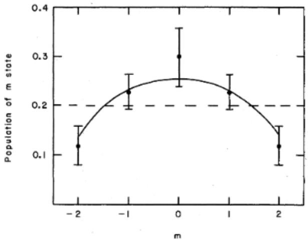

FIG. 9. The points are the calculated populations of the various m substates of the 2^+ level in ^{144}Ba. These values were determined using the fitted experimental angular distribution of the $2^+ \to 0^+$ γ ray. The solid line represents the predicted population of the m states as calculated from the statistical-model analysis of the de-excitation process using Eqs. (4) and (5) with an assumed value of $B = 6$ [Eq. (3)] for the initial angular momentum distribution.

J. B. Wilhelmy, E. Cheifetz, R. C. Jared, S. G. Thompson, H. R. Bowman, and J. O. Rasmussen Phys. Rev. C 5, 2041 (1972)

Literature

- Thermal excitations
- Quantum fluctuations
- Coulomb force
- Breaking of the neck

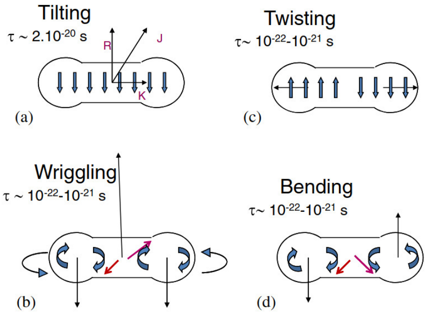

Illustration from B. John, J. Phys., 85, 2, (2015).

Pair breaking mechanism ?

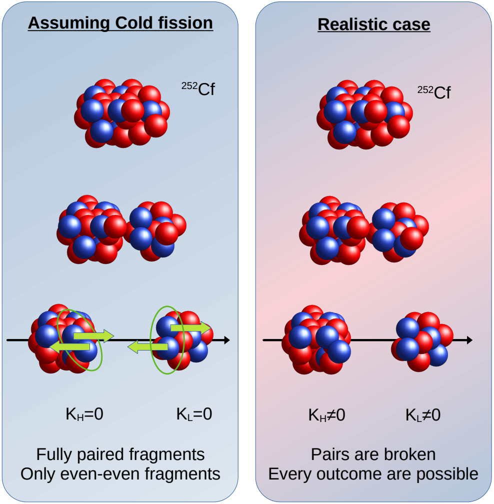

Vanishing pairing during dynamics ?

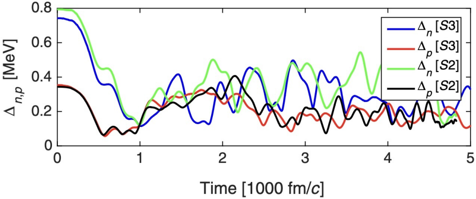

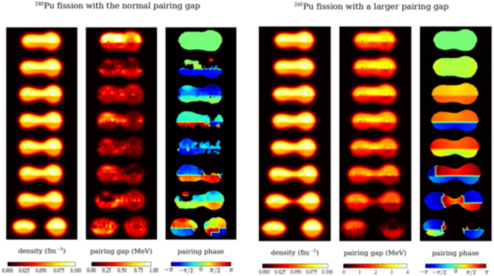

A. Bulgac, P. Magierski, Kenneth J. Roche, and I. Stetcu, PRL 116, 122504 (2016).

Projection method

Projection on the spin and K number (Projection of the spin on the fission axis)

$$\hat{P}^{S}_{MK} = \frac{(2S+1)}{16\pi^2} \int d\Omega \mathcal{D}^{S*}_{MK}(\Omega)\, e^{i\alpha\hat{S}_z} e^{i\beta\hat{S}_y} e^{i\gamma\hat{S}_z},$$

$$P(S_F, K_F) = \langle\Psi|\hat{P}^{S_F}_{K_F K_F}|\Psi\rangle,$$

Calculation of the overlap : G. F. Bertsch and L. M. Robledo, PRL 108, 042505 (2012)

$$\langle\Psi|\hat{R}|\Psi\rangle = \frac{(-1)^n}{\prod_\alpha^n v_\alpha^2} \mathrm{pf}\begin{bmatrix} V^T U & V^T R^T V^* \\ -V^\dagger R V & U^\dagger V^* \end{bmatrix}$$

Optimized Pfaffian calculation : M. Wimmer, ACM Trans. Math Softw. 38, 30 (2012).

Pair breaking mechanism ?

Spin distribution in the fragments

Obtained using 3-angle projection operator

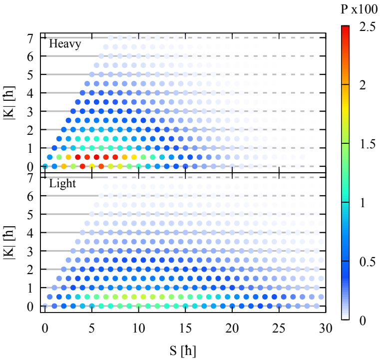

TDHFB - SEALL1

Geometry of the reaction

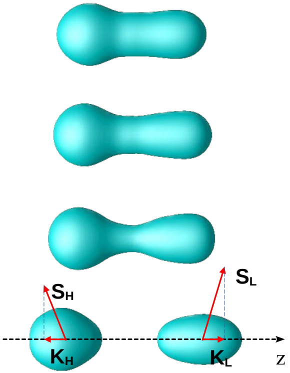

G.scamps, I. Abdurrahman, M. Kafker, A. Bulgac, and I. Stetcu, PRC 108 (6), L061602

Pair breaking mechanism ?

Assuming Cold fission

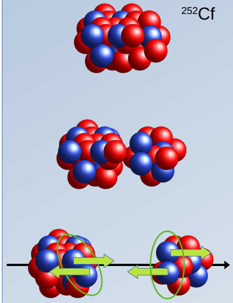

$K_H=0$ $K_L=0$

Fully paired fragments
Only even-even fragments

Realistic case

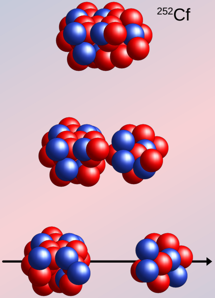

$K_H \neq 0$ $K_L \neq 0$

Pairs are broken
Every outcome are possible

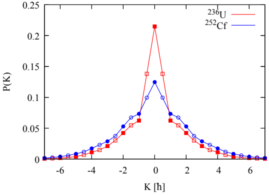

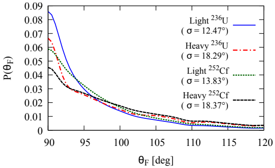

$$\cos \theta_F = \frac{K_F}{\sqrt{S_F(S_F+1)}}$$

G.scamps, I. Abdurrahman, M. Kafker, A. Bulgac, and I. Stetcu, PRC 108 (6), L061602.

Orbital angular momemtum

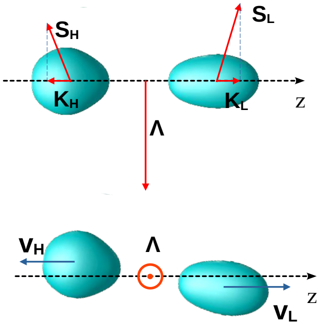

In spontaneous fission of a 0^+ state

$$\mathbf{S_H} + \mathbf{S_L} + \mathbf{\Lambda} = \mathbf{0},$$

Triangular rule :

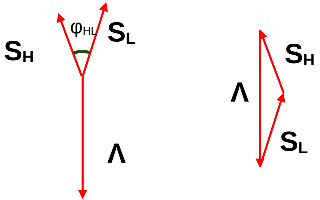

$$\cos(\varphi_{HL}) = \left(\frac{\Lambda(\Lambda+1) - S_H(S_H+1) - S_L(S_L+1)}{2\sqrt{S_H(S_H+1)S_L(S_L+1)}} \right)$$

TDDFT (in 2022) vs Freya

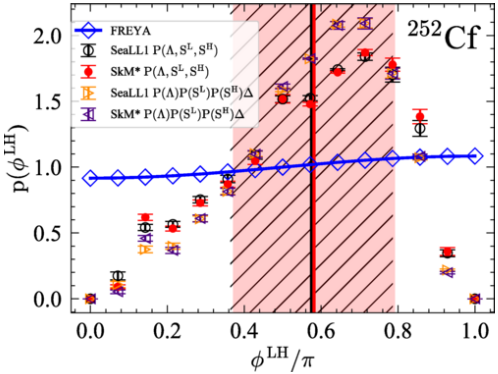

A. Bulgac, I. Abdurrahman, K. Godbey, and I. Stetcu, Phys. Rev. Lett. 128, 022501(2022).

Opening angle distribution

$$\varphi_{HL} = \arccos\left(\frac{\Lambda(\Lambda+1) - S_H(S_H+1) - S_L(S_L+1)}{2\sqrt{S_H(S_H+1)S_L(S_L+1)}}\right)$$

$$P(\Lambda, S_H, S_L) = \sum_{k_H k_L} \langle\Psi|\hat{P}^{\Lambda}_{0,0}\hat{P}^{S_H}_{K_H K_H}\hat{P}^{S_L}_{K_L K_L}|\Psi\rangle.$$

$$P(\Lambda, S_H, S_L) = \sum_{K_H K_L K'_H K'_L} (-1)^{K'_H - K_H + K'_L - K_L}$$

$$C^{\Lambda,0}_{S_H,-K_H,S_L,-K_L} C^{\Lambda,0}_{S_H,-K'_H,S_L,-K'_L} \langle\Psi|\hat{P}^{S_H}_{K_H K'_H}\hat{P}^{S_L}_{K_L K'_L}|\Psi\rangle$$

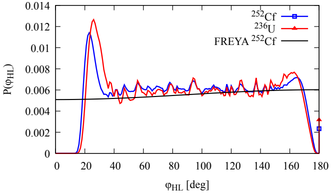

G.scamps, I. Abdurrahman, M. Kafker, A. Bulgac, and I. Stetcu, PRC 108 (6), L061602.

One angle projector :

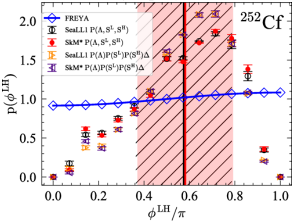

Opening angle distribution

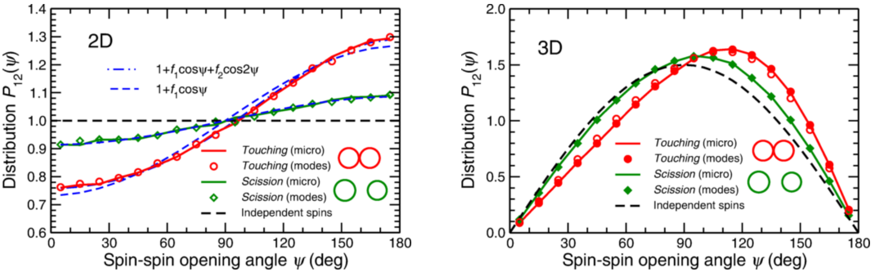

J. Randrup, Phys. Rev. C 106, L051601 (2022).

Question

- How the quantal effects change this picture ?
- How the geometry change the opening angle distribution assuming no correlation ?

Opening angle distribution - why the spins can not be aligned ?

Non alignement of the spins

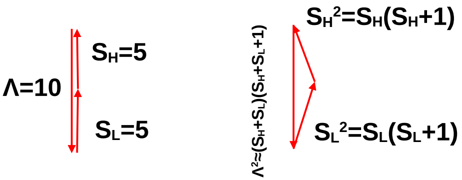

To get a 5 degrees angle between two spins require spins of 262 $\hbar$ and 6565 $\hbar$ for 1 degree

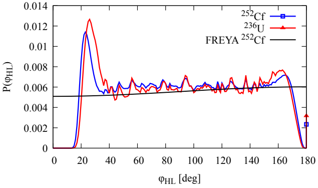

Non alignement of the spins

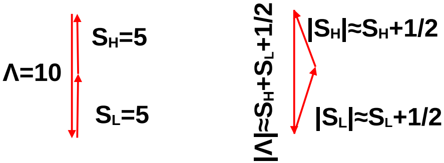

To get a 5 degrees angle between two spins require spins of 262 $\hbar$ and 6565 $\hbar$ for 1 degree

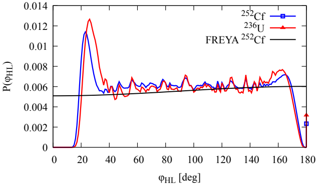

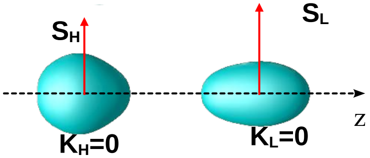

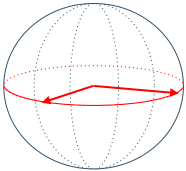

$$|\Psi\rangle = \sum_{S_H,K_H,S_L,K_L} c_{S_H,K_H,S_L,K_L} |S_H, K_H, S_L, K_L\rangle,$$

$$|c_{S_H,K_H,S_L,K_L}|^2 \propto \delta_{K_H,0}\delta_{K_L,0}(2S_H+1)e^{\frac{-S_H(S_H+1)}{2\sigma_H^2}} \times (2S_L+1)e^{\frac{-S_L(S_L+1)}{2\sigma_L^2}}.$$

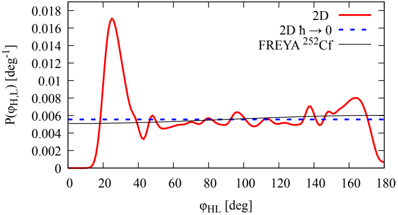

G. Scamps, PRC 109, L011602 (2024).

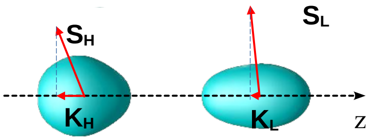

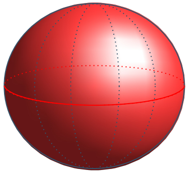

$$|\Psi\rangle = \sum_{S_H,K_H,S_L,K_L} c_{S_H,K_H,S_L,K_L} |S_H, K_H, S_L, K_L\rangle,$$

$$|c_{S_H,K_H,S_L,K_L}|^2 \propto e^{\frac{-S_H(S_H+1)}{2\sigma_H^2}} e^{\frac{-S_L(S_L+1)}{2\sigma_L^2}}.$$

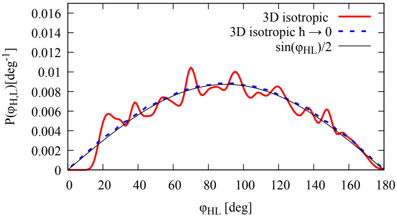

G. Scamps, PRC 109, L011602 (2024).

Opening angle distribution - 3D from TDDFT

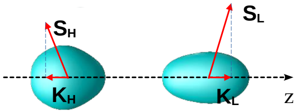

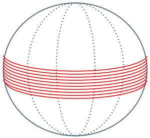

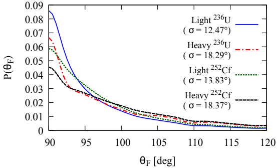

$$|\Psi\rangle = \sum_{S_H,K_H,S_L,K_L} c_{S_H,K_H,S_L,K_L} |S_H, K_H, S_L, K_L\rangle,$$

$|c_{S_H,K_H,S_L,K_L}|^2$ From TDDFT

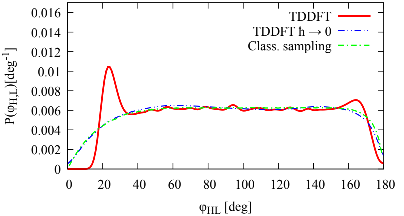

TDDFT shows an intermediate case between 2D and 3D.
G. Scamps, PRC 109, L011602 (2024).

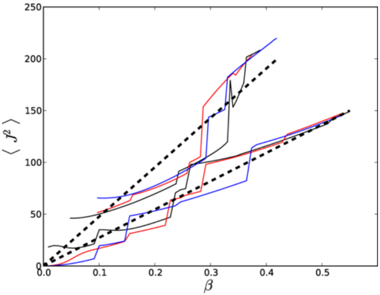

G. F. Bertsch, T. Kawano, and L. M. Robledo, PRC 99, 034603 (2019)

Problem of interpretation

- The spin cut-off distribution is already present in the ground state of even-even deformed nuclei if symmetry are not restored
- $\hat{J}^2$ and $\hat{P}(J)$ are 2 and N-body operators
- Fragments do not rotate in dynamical approaches

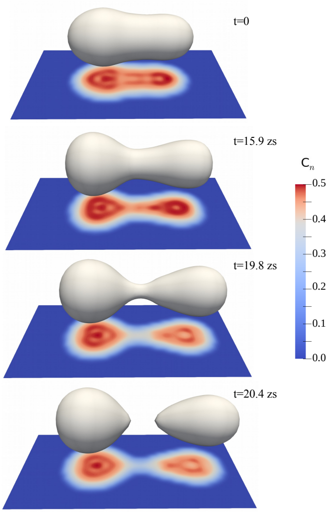

Problem of interpretation

- The spin cut-off distribution is already present in the ground state of even-even deformed nuclei if symmetry are not restored
- $\hat{J}^2$ and $\hat{P}(J)$ are 2 and N-body operators
- Fragments do not rotate in dynamical approaches

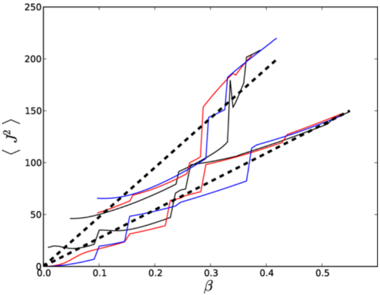

G. F. Bertsch, T. Kawano, and L. M. Robledo, PRC 99, 034603 (2019)

Problem of interpretation

- The spin cut-off distribution is already present in the ground state of even-even deformed nuclei if symmetry are not restored
- $\hat{J}^2$ and $\hat{P}(J)$ are 2 and N-body operators
- Fragments do not rotate in dynamical approaches

Uncertainty principle ?

If the overlap is gaussian

$$\langle\Psi|\hat{R}(\theta)|\Psi\rangle = e^{-\frac{\theta^2}{2\sigma_\theta^2}}$$

The projection gives,

$$P(J) = \frac{2J+1}{2{\sigma_J}^2} e^{-\frac{J(J+1)}{2\sigma_J^2}}$$

with $\sigma_J \sigma_\theta = 1$

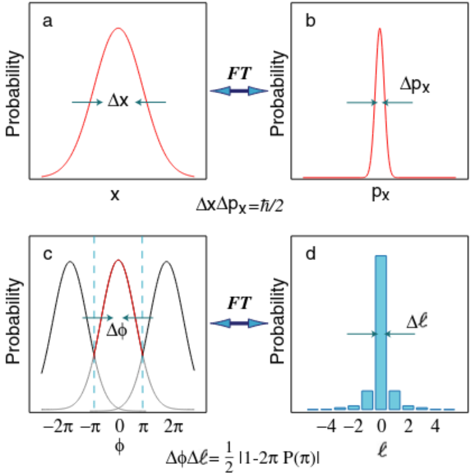

S. Franke-Arnold, et al. New Journal of Physics 6, 103 (2004)

G. Scamps, G. Bertsch, Phys. Rev. C 108, 034616(2023).

Orientation pumping mechanism

Isotropic potential at scission

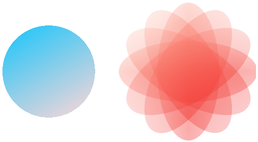

Confining potential at scission

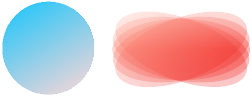

L. Bonneau, P. Quentin, and I. N. Mikhailov, PRC 75, 064313 (2007).

For $\Delta\Theta = 1^\circ$, $\Delta L = 56\hbar$.

For a nucleus, angular velocity $\omega = 10^{20} s^{-1}$

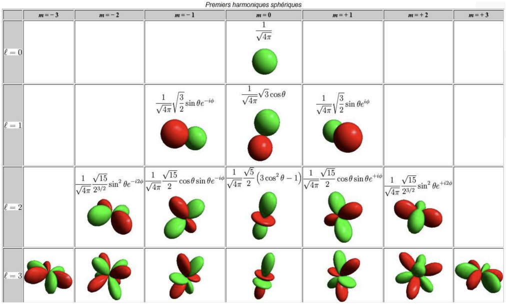

G. Scamps, G. Bertsch, Phys. Rev. C 108, 034616(2023).

Orientation pumping mechanism

<u>Isotropic potential at scission</u>

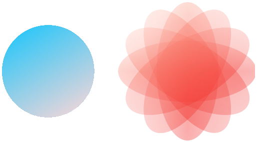

<u>Confining potential at scission</u>

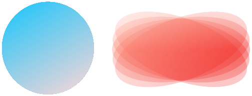

L. Bonneau, P. Quentin, and I. N. Mikhailov, PRC 75, 064313 (2007).

For $\Delta\Theta = 1^\circ$, $\Delta L = 56\hbar$.

For a nucleus, angular velocity $\omega = 10^{20} s^{-1}$

Main points

- Internal excitation (breaking of pairs)
- Spins are mainly perpendicular to the fission axis
- Uncorrelated magnitude and orientation of the spins

Outlook

- TD-GCM with rotated fragments
- Rotated fission system

Thank you

^{144}Ba + ^{96}Sr at 16 Fm, Θ_{ini}=25 deg, Functional : Skyrme Sly4d

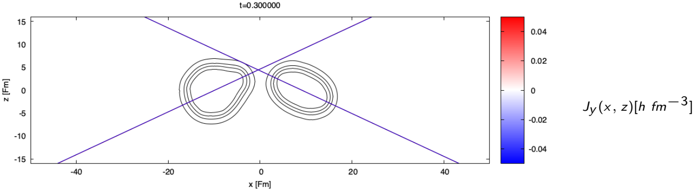

G. Scamps, PRC 106, 054614 (2022).

One body-evolution - One body-observable

^{144}Ba + ^{96}Sr at 16 Fm, Θ_{ini}=25 deg, Functional : Skyrme Sly4d

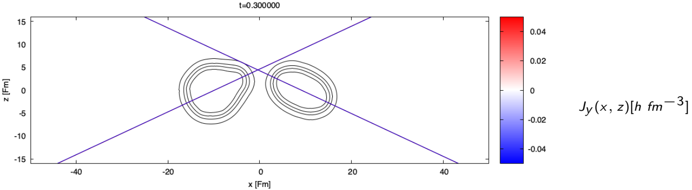

G. Scamps, PRC 106, 054614 (2022).

One body-evolution - One body-observable

Microscopic DFT calculations

Static HFB

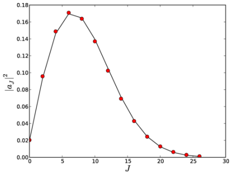

G. F. Bertsch, T. Kawano, and L. M. Robledo, PRC 99, 034603 (2019)

Scission configuration

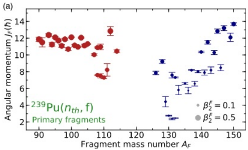

P. Marević, N. Schunck, J. Randrup, and R. Vogt PRC 104, L021601 (2021).

TDHFB - TDSLDA

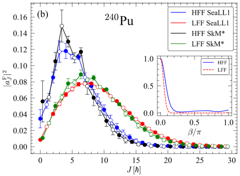

A. Bulgac, et al., PRL 126, 142502 (2021)

Projection method

$$\hat{P}_J \left(|\Psi(J=0)\rangle + |\Psi(J=1)\rangle + \ldots \right) = |\Psi(J)\rangle$$

$$|a_J^F|^2 = \frac{2J+1}{2} \int_0^{2\pi} \sin(\beta) \, P_J(\cos(\beta)) \langle \Psi | e^{\frac{-i\hat{J}_x^F \beta}{\hbar}} | \Psi \rangle$$

^{144}Ba + ^{96}Sr at 16 Fm, Θ_{ini}=25 deg, Functional : Skyrme Sly4d

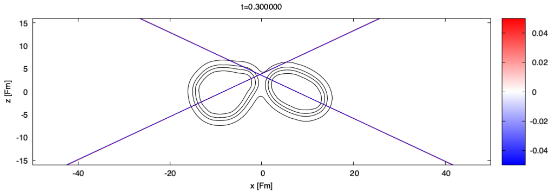

$J_y(x,z)[h\ fm^{-3}]$

G. Scamps, PRC 106, 054614 (2022).

^{144}Ba + ^{96}Sr at 16 Fm, Θ_{ini}=25 deg, Functional : Skyrme Sly4d

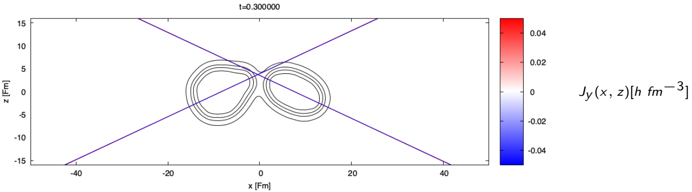

G. Scamps, PRC 106, 054614 (2022).

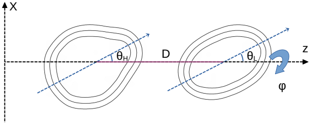

Potential as a function of the light fragment angle

$^{132}Sn+^{108}Ru$

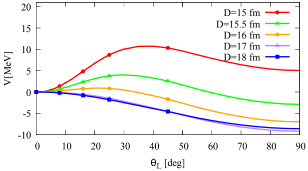

Two torques :

- attractive nucleus-nucleus torque
- repulsive Coulomb torque

Potential as a function of the light fragment angle

$^{144}Ba+^{96}Sr$. D=15.5 and 20 fm

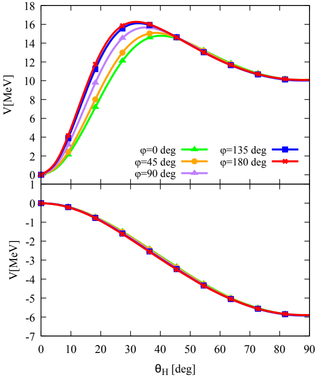

The azimuthal angle doesn't have an important role.

Frozen Hartree-Fock potential

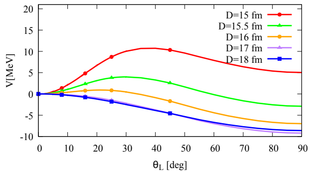

Two torques :

- attractive nucleus-nucleus torque
- repulsive Coulomb torque

4 degrees of freedom

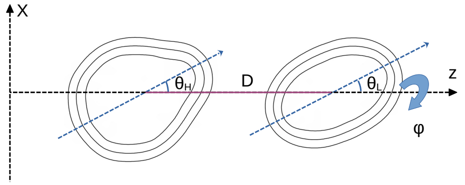

Hamiltonian

$$\hat{H}(D) = \frac{\hbar^2}{2I_H}\hat{L}_H^2 + \frac{\hbar^2}{2I_L}\hat{L}_L^2 + \frac{\hbar^2}{2I_\Lambda(D)}\hat{\Lambda}^2 + \hat{V}(\hat{\Theta}_H, \hat{\Theta}_L, \hat{\varphi}, D)$$

Solved in basis $|L_H, m, L_L, -m\rangle$

G. Scamps, G. Bertsch, Phys. Rev. C 108, 034616(2023).
Similar to the orientation pumping mechanism model Mikhailov, I. N., and Quentin, P. Physics Letters B, 462(1-2), 7-13 (1999)

Evolution of a one-angle wave packet assuming spherical ^{132}Sn

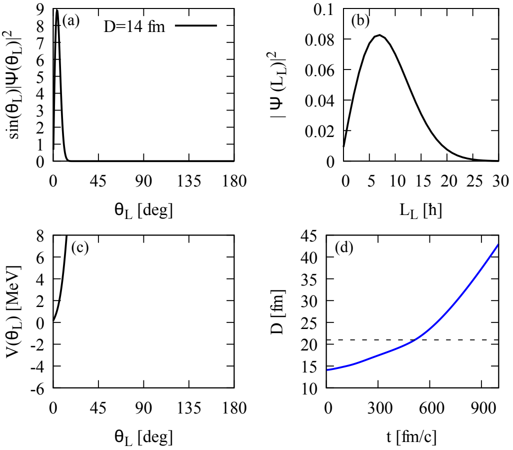

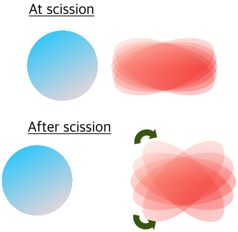

G. Scamps, G. Bertsch, Phys. Rev. C 108, 034616 (2023).

Evolution of a one-angle wave packet assuming spherical ^{132}Sn

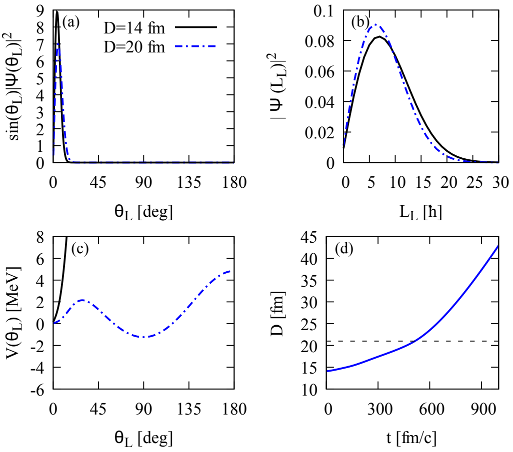

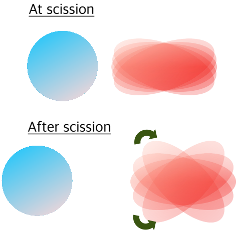

G. Scamps, G. Bertsch, Phys. Rev. C 108, 034616 (2023).

Evolution of a one-angle wave packet assuming spherical ^{132}Sn

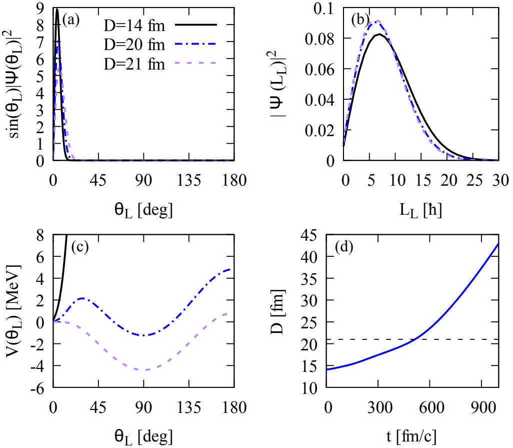

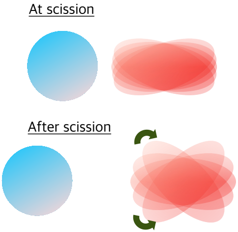

G. Scamps, G. Bertsch, Phys. Rev. C 108, 034616 (2023).

Evolution of a one-angle wave packet assuming spherical ^{132}Sn

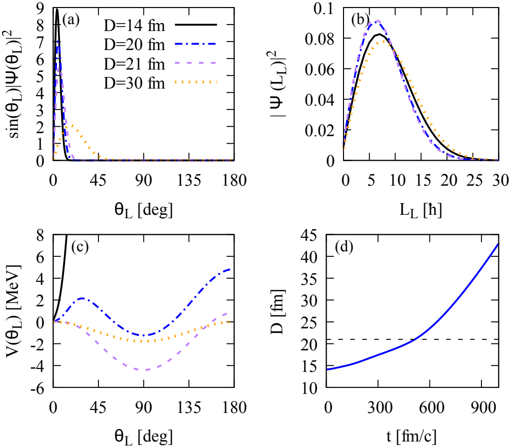

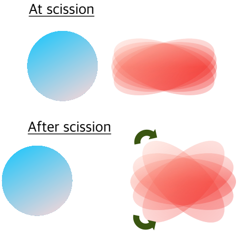

G. Scamps, G. Bertsch, Phys. Rev. C 108, 034616 (2023).

Evolution of a one-angle wave packet assuming spherical ^{132}Sn

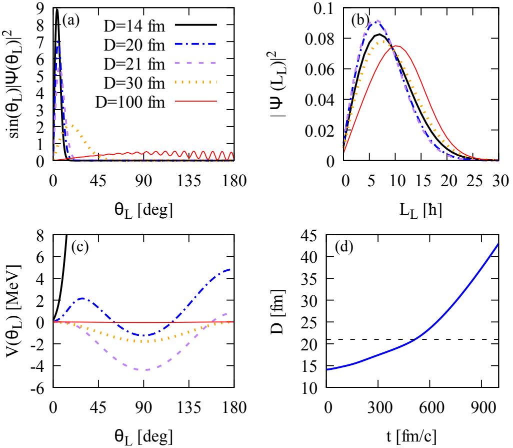

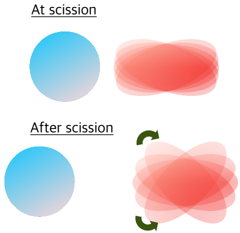

G. Scamps, G. Bertsch, Phys. Rev. C 108, 034616 (2023).

Effect of quadrupole deformation $>>$ effect of $Z_1 Z_2$

TABLE II. Average spin$\langle L^2 \rangle^{\frac{1}{2}}$ in unit of $\hbar$ for the three fission fragments at scission ($D = 21$ fm) and at large distances. The last two columns show the same quantity with an MOI divided by 2.

Nucleus	Scission	Final	Scission ($I_{\frac{1}{2}}$)	Final ($I_{\frac{1}{2}}$)
^{108}Ru	9.28	12.31	7.24	10.38
^{144}Ba	10.04	10.95	7.70	8.66
^{96}Sr	7.74	9.30	6.03	7.62

also J. Randrup, PRC 108, 064606 (2023) : increase of 1 to 3 $\hbar$ due to the Coulomb torque.

Cold fission selection TXE<8MeV

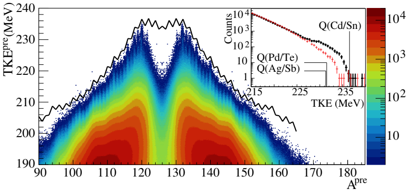

γ-spectrum

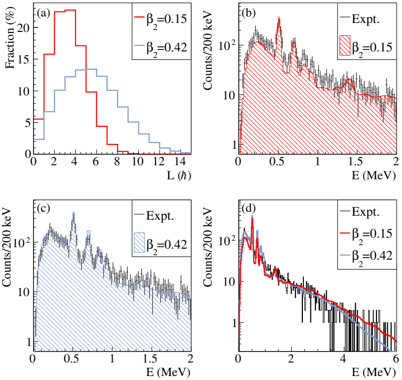

Results

- ^{132}Sn is found in ground-state
- The collective Hamiltonian model with β_2=0.42 reproduces the experimental γ-spectrum

A. Francheteau, L. Gaudefroy, G. Scamps, O. Roig, V. Méot, A. Ebran, and G. Bélier, PRL 132, 142501 (2024).

Correlation between the angular momentum

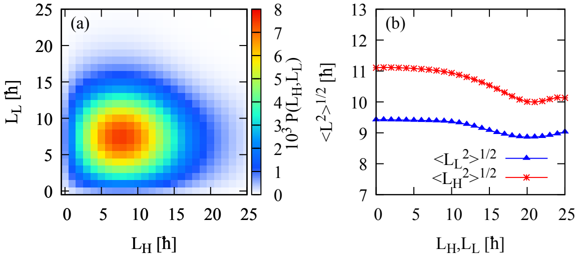

$^{144}Ba+^{96}Sr$

- No or small correlation observed in the magnitude of the angular momentum.
- More angular momentum for the heavy fragment

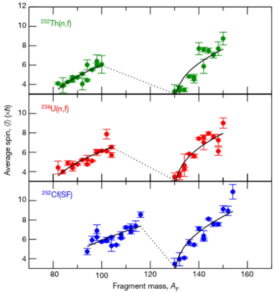

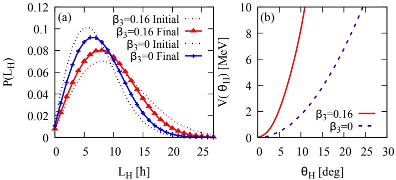

G. Scamps, G. Bertsch, Phys. Rev. C 108, 034616 (2023).

Mechanism

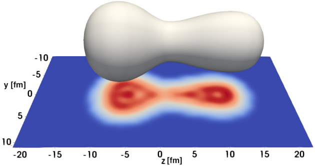

- Pear-shaped deformation plays an important role at scission. G. Scamps C. Simenel, Nature 564, pages 382–385 (2018)
- Octupole deformation makes the angular potential stiffer which increase the zero-point motion → more angular momentum

Orbital angular momemtum

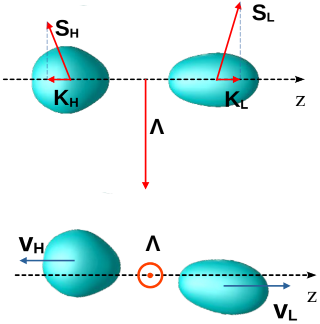

In spontaneous fission of a 0^+ state

$$\mathbf{S_H} + \mathbf{S_L} + \mathbf{\Lambda} = \mathbf{0},$$

Triangular rule :

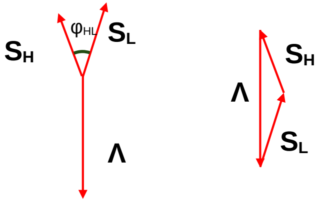

$$\cos(\varphi_{HL}) = \left(\frac{\Lambda(\Lambda+1) - S_H(S_H+1) - S_L(S_L+1)}{2\sqrt{S_H(S_H+1)S_L(S_L+1)}} \right)$$

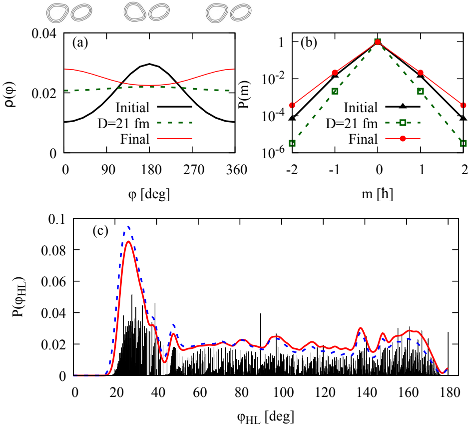

G. Scamps, G. Bertsch, Phys. Rev. C 108, 034616 (2023).

Geometry

- Small azimuthal correlation
- Spins are perpendicular to the fission axis
- Complex pattern in the opening angle, different from previous model

Outlook : Case where total spin is not zero

^{208}Pb+^{208}Pb

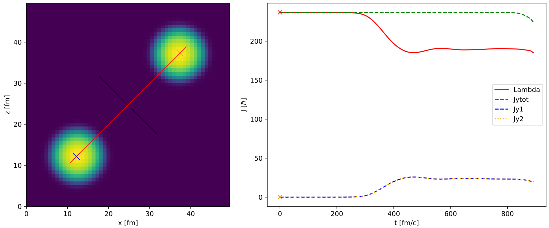

^{50}Ca+^{176}Yb

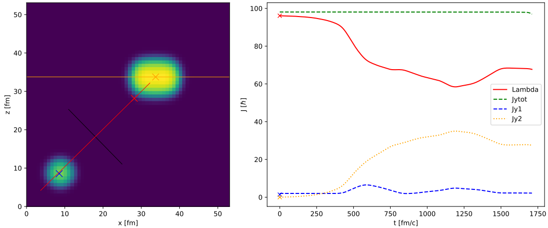

G. Scamps, Microscopic Study of Spin Transfer in Near-Barrier Nuclear Reactions, Phys. Rev. C 110, 054605 (2024).

Outlook : Case where total spin is not zero

$^{208}Pb+^{208}Pb$

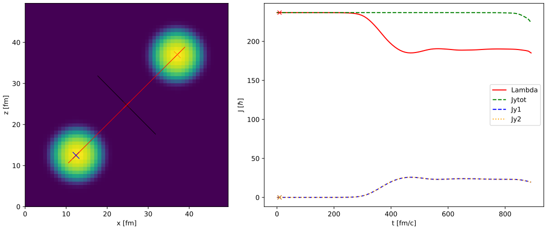

$^{50}Ca+^{176}Yb$

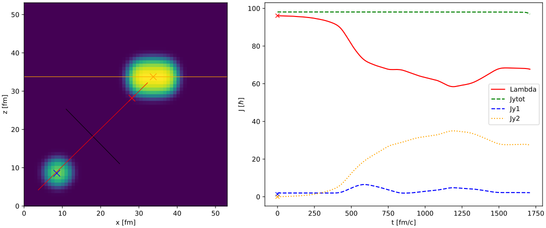

G. Scamps, Microscopic Study of Spin Transfer in Near-Barrier Nuclear Reactions, Phys. Rev. C 110, 054605 (2024).

Outlook : Case where total spin is not zero

^{208}Pb+^{208}Pb

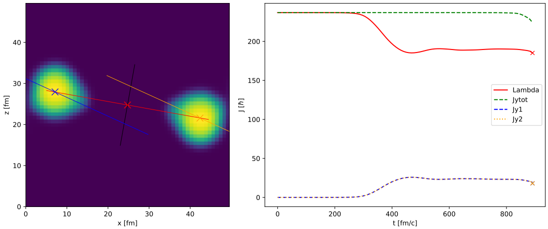

^{50}Ca+^{176}Yb

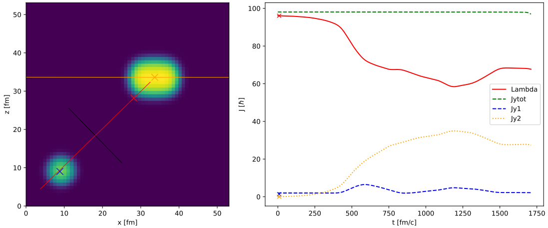

G. Scamps, Microscopic Study of Spin Transfer in Near-Barrier Nuclear Reactions, Phys. Rev. C 110, 054605 (2024).